Electronic Supplementary Material (ESI) for Molecular Systems Design & Engineering.
This journal is © The Royal Society of Chemistry 2019

Towards Efficient Initiators for Two-Photon Induced Polymerization: Fine Tuning of the Donor/Acceptor Properties

Brigitte Holzer,[†*] *Markus Lunzer,*[†,‡] *Arnulf Rosspeintner,*[§] *Giuseppe Licari,*[§] *Maximilian Tromayer,*[†,‡] *Sergej Naumov,*[#] *Daniel Lumpi,*[†] *Ernst Horkel,*[†] *Christian Hametner,*[†] *Aleksandr Ovsianikov,*[‡] *Robert Liska,*[†] *Eric Vauthey*[§] *and Johannes Fröhlich*[†]

[†]Institute of Applied Synthetic Chemistry, TU Wien, Getreidemarkt 9/163, A-1060 Vienna, Austria

[§]Department of Physical Chemistry, University of Geneva, 30 Quai Ernest-Ansermet, CH-1211 Geneva, Switzerland

[‡]Institute of Materials Science and Technology, TU Wien, Getreidemarkt 9/308, A-1040 Vienna, Austria

[#]Leibniz Institute of Surface Engineering (IOM), Permoserstrasse 15, D-04318 Leipzig, Germany

*brigitte.holzer@tuwien.ac.at

A) Synthesis

Materials and Characterization Techniques. Substances purchased from commercial sources were used as received without further purification. 4-Fluorobenzonitrile was purchased from ABCR GmbH. Allyl[1,3-bis(2,6-diisopropylphenyl)imidazol-2-ylidene]chloropalladium(II) ((IPr)Pd(allyl)Cl, CAS 478980-03-9),[1] 1-fluoro-4-(methylsulfonyl)benzene (CAS 455-15-2),[2] 4,4'-(2,5-thiophenediyl)bis(benzenamine) (**3**, CAS 70010-49-0)[3] and all applied boronic esters[4] were synthesized according to literature. Isopropyl alcohol (IPA) and dimethyl sulfoxide (DMSO) were used in p.a. quality. Technical grade solvents were distilled prior to use. For spectroscopic measurements acetonitrile (ACN) (Roth, Rotidry, ≥ 99.9%), tetrahydrofuran (THF) (VWR, 99.7%, Chromanorm), n-hexane (n-Hex) (Roth, Rotidry, ≥ 99%) and methanol (MeOH) (Sigma-Aldrich, ≥ 99.9%, spectrophotometric grade) were used as received. Coumarin 485 (Exciton), Coumarin 153 (Radiant Dyes) and LDS 698 (Exciton) were used as received. Nuclear magnetic resonance (NMR) spectra were obtained using a Bruker DPX-200 or Avance DRX-400 fourier transform spectrometer operating at the following frequencies: DPX-200: 200.1 MHz (^{1}H) and 50.3 MHz (^{13}C); DRX-400: 400.1 MHz (^{1}H) and 100.6 MHz (^{13}C). The chemical shifts are reported in delta (δ) units, parts per million (ppm) downfield from tetramethylsilane using residual solvent signals for calibration. Coupling constants are reported in Hertz; multiplicity of signals is indicated by using following abbreviations: s = singlet, d = doublet, t = triplet, q = quartet. The multiplicity of ^{13}C signals was obtained by measuring JMOD spectra. Melting points (m_p) were recorded on an OptiMelt Automated Melting Point System (Stanford Research Systems) and are corrected.

High-resolution mass spectra (HRMS) were acquired as radical cations using either a SYNAPT HDMS instrument (Waters, Manchester, UK) equipped with a matrix-assisted laser desorption/ionization (MALDI) source or a Thermo Scientific LTQ Orbitrap XL hybrid FTMS (Fourier Transform Mass Spectrometer) equipped with Thermo Fischer Exactive Plus Orbitrap (LC-ESI$^+$) and a Shimadzu IT-TOF Mass Spectrometer. Samples for MALDI-HRMS were applied at 1 mg mL^{-1} in THF on stainless steel using nitroanthracene (3 mg mL^{-1} in THF) as MALDI matrix. All

MS spectra were recorded as accurate mass data with angiotensin II (m/z = 1046.542) as internal lock mass achieving a mass accuracy of 15–40 ppm (i.e. Δm/z = 0.01–0.04 amu).

Synthesis. Analytical TLC was performed on Merck silica gel 60 F254 plates. Chromatographic separations at preparative scale were carried out on silica gel (Merck silica gel 60, 40–63 μm).

General procedure for the synthesis of **BMOA-1T, BtBuA-1T, BMA-1T, BHA-1T, BTMSA-1T** and **BFA-1T** according to Marion *et al.*[5] Under an argon atmosphere, 2,5-dibromothiophene **2** (1.0 eq.), boronic ester (3.0 eq.) and KOtBu (3.0 eq.) were suspended in 16 mL solvent (IPA : H_2O, 3 : 1; degassed by bubbling with argon). A solution of (IPr)Pd(allyl)Cl (0.02 eq.) in degassed IPA was added and the reaction mixture was refluxed for 1.5 hours, monitoring the conversion by TLC. After completion, the reaction mixture was distributed between water and chloroform; the phases were separated, and the aqueous layer was extracted with chloroform three times. The combined organic layer was dried over anhydrous sodium sulfate and the solvent removed under reduced pressure to give the crude product. Purification was achieved by column chromatography.

4,4'-(2,5-Thiophenediyl)bis[*N,N*-bis(4-methoxyphenyl)benzenamine] (**BMOA-1T**). According to the general procedure **BMOA-1T** was synthesized applying 2,5-dibromothiophene **2** (242 mg, 1 mmol), boronic acid pinacol ester **1a** (1294 mg, 3.0 mmol), KOtBu (337 mg, 3.0 mmol) and (IPr)Pd(allyl)Cl (11.4 mg, 20 μmol; dissolved in 1 mL IPA). After general workup the crude product was purified by column chromatography (90 g silica gel, hexanes : Et_2O 30 to 100%) and subsequently recrystallized from cyclohexane to give **BMOA-1T** as yellow powder (647 mg, 94%). ^{1}H NMR (400 MHz, CD_2Cl_2): δ = 7.42 (d, *J* = 8.8 Hz, 4 H), 7.13 (s, 2 H), 7.10 - 7.04 (m, 8 H), 6.93 - 6.82 (m, 12 H), 3.79 (s, 12 H) ppm. ^{13}C NMR (100 MHz, CD_2Cl_2): δ = 156.7 (s), 148.7 (s), 142.9 (s), 141.1 (s), 127.3 (d), 127.0 (s), 126.5 (d), 123.1 (d), 120.9 (d), 115.2 (d), 56.0 (q) ppm. R_f = 0.55 (DCM : methanol 6 : 1). MS (MALDI-TOF): calcd for $C_{44}H_{38}N_2O_4S$: 690.2552; found: 690.2450.

4,4'-(2,5-Thiophenediyl)bis[*N,N*-bis[4-(1,1-dimethylethyl)phenyl]-benzenamine] (**BtBuA-1T**). According to the general procedure **BtBuA-1T** was synthesized applying 2,5-dibromothiophene **2** (242 mg, 1 mmol), boronic acid pinacol ester **1b** (1451 mg, 3.0 mmol), KOtBu (337 mg, 3.0 mmol) and (IPr)Pd(allyl)Cl (11.4 mg, 20 μmol; dissolved in 1 mL IPA). After general workup the crude product was purified by column chromatography (90 g silica gel, cyclohexane : DCM, 9 to 17 %) and subsequently recrystallized from cyclohexane to give **BtBuA-1T** as yellow powder (724 mg, 91%). ^{1}H NMR (400 MHz, CD_2Cl_2): δ = 7.46 (d, *J* = 8.6 Hz, 4 H), 7.30 (d, *J* = 8.6 Hz, 8 H), 7.18 (s, 2 H), 7.04 - 7.00 (m, 12 H), 1.32 (s, 36 H) ppm. ^{13}C NMR (100 MHz, CD_2Cl_2): δ = 148.2 (s), 146.8 (s), 145.4 (s), 143.1 (s), 128.1 (s), 126.7 (d), 126.6 (d), 124.8 (d), 123.4 (d), 123.1 (d), 34.8 (s), 31.7 (q) ppm. R_f = 0.27 (light petrol : DCM 10 : 1). MS (MALDI-TOF): calcd for $C_{56}H_{62}N_2S$: 794.4634; found: 794.4633.

4,4'-(2,5-Thiophenediyl)bis[*N*,*N*-bis(4-methylphenyl)benzenamine] (**BMA-1T**). According to the general procedure **BMA-1T** was synthesized applying 2,5-dibromothiophene **2** (242 mg, 1 mmol), boronic acid pinacol ester **1c** (1198 mg, 3.0 mmol), KOtBu (337 mg, 3.0 mmol) and (IPr)Pd(allyl)Cl (11.4 mg, 20 μmol; dissolved in 1 mL IPA). After general workup the crude product was purified by column chromatography (90 g silica gel, cyclohexane : DCM, 7 to 14%) and subsequently recrystallized from cyclohexane to give **BMA-1T** as yellow powder (551 mg, 88%). ^{1}H NMR (400 MHz, CD_2Cl_2): δ = 7.44 (d, J = 8.7 Hz, 4 H), 7.16 (s, 2 H), 7.10- 7.08 (m, 8 H), 7.00- 6.96 (m, 12 H), 2.32 (s, 12 H) ppm. ^{13}C NMR (100 MHz, CD_2Cl_2): δ = 148.3 (s), 145.6 (s), 143.1 (s), 133.6 (s), 130.5 (d), 128.0 (s), 126.6 (d), 125.3 (d), 123.4 (d), 122.8 (d), 21.1 (q) ppm. R_f = 0.19 (light petrol : DCM 10 : 1). Mp = 206.1 – 210.7 °C. MS (MALDI-TOF): calcd for $C_{44}H_{38}N_2S$: 626.2756; found: 626.2672.

4,4'-(2,5-Thiophenediyl)bis[*N*,*N*-bis[4-(trimethylsilyl)phenyl]-benzenamine] (**BTMSA-1T**). According to the general procedure **BTMSA-1T** was synthesized applying 2,5-dibromothiophene **2** (242 mg, 1 mmol), boronic acid pinacol ester **1d** (1547 mg, 3.0 mmol), KOtBu (337 mg, 3.0 mmol) and (IPr)Pd(allyl)Cl (11.4 mg, 20 μmol; dissolved in 1 mL IPA). After general workup the crude product was purified by column chromatography (90 g silica gel, cyclohexane : DCM, 9 to 17 %) and subsequently recrystallized from cyclohexane to give **BTMSA-1T** as yellow powder (705 mg, 82%). ^{1}H NMR (400 MHz, CD_2Cl_2): δ = 7.51 (d, *J* = 8.4 Hz, 4 H), 7.42 (d, *J* = 8.2 Hz, 8 H), 7.22 (s, 2 H), 7.09 - 7.07 (m, 12 H), 0.26 (s, 36 H) ppm. ^{13}C NMR (100 MHz, CD_2Cl_2): δ = 148.4 (s), 147.4 (s), 143.2 (s), 135.0 (s), 134.9 (d), 129.3 (s), 126.8 (d), 124.9 (d), 124.0 (d), 123.9 (d), -0.8 (q) ppm. R_f = 0.18 (light petrol : DCM 10 : 1). MS (MALDI-TOF): calcd for $C_{52}H_{62}N_2SSi_4$: 858.3711; found: 858.3618.

4,4'-(2,5-Thiophenediyl)bis[*N,N*-diphenylbenzenamine] (**BHA-1T**). According to the general procedure **BHA-1T** was synthesized applying 2,5-dibromothiophene **2** (242 mg, 1 mmol), boronic acid pinacol ester **1e** (1114 mg, 3.0 mmol), KOtBu (337 mg, 3.0 mmol) and (IPr)Pd(allyl)Cl (11.4 mg, 20 μmol; dissolved in 1 mL IPA). After general workup the crude product was purified by column chromatography (90 g silica gel, cyclohexane : DCM, 5 to 10%) and subsequently recrystallized from cyclohexane to give **BHA-1T** as yellow powder (525 mg, 92%). ^{1}H NMR (400 MHz, CD_2Cl_2): δ = 7.49 (d, *J* = 8.5 Hz, 4 H), 7.30 - 7.26 (m, 8 H), 7.21 (s, 2 H), 7.12 - 7.10 (m, 8 H), 7.10 - 7.03 (m, 8 H) ppm. ^{13}C NMR (100 MHz, CD_2Cl_2): δ = 148.1 (s), 147.8 (s), 143.1 (s), 129.9 (d), 128.9 (s), 126.8 (d), 125.1 (d), 124.2 (d), 123.7 (d), 123.7 (d) ppm. R_f= 0.24 (light petrol : DCM 10 : 1). Mp = 192.2 – 193.3 °C. MS (MALDI-TOF): calcd for $C_{40}H_{30}N_2S$: 570.2130; found: 570.1812.

4,4'-(2,5-Thiophenediyl)bis[*N,N*-bis(4-fluorophenyl)benzenamine] (**BFA-1T**). According to the general procedure **BFA-1T** was synthesized applying 2,5-dibromothiophene **2** (242 mg, 1 mmol), boronic acid pinacol ester **1f** (1222 mg, 3.0 mmol), KOtBu (337 mg, 3.0 mmol) and (IPr)Pd(allyl)Cl (11.4 mg, 20 μmol; dissolved in 1 mL IPA). After general workup the crude product was purified by column chromatography (90 g silica gel, cyclohexane : DCM, 15 to 20%) and subsequently recrystallized from cyclohexane to give **BFA-1T** as yellow powder (590 mg, 92%). ^{1}H NMR (400 MHz, CD_2Cl_2): δ = 7.48 (d, *J* = 8.8 Hz, 4 H), 7.18 (s, 2 H), 7.14 - 6.90 (m, 20 H) ppm. ^{13}C NMR (100 MHz, CD_2Cl_2): δ = 159.6 (s, J_{CF} = 243.2 Hz), 147.9 (s), 144.1 (s, J_{CF} = 2.8 Hz), 143.0 (s), 128.6 (s), 126.9 (d, J_{CF} = 7.9 Hz), 126.8 (d), 123.7 (d), 123.0 (d), 116.7 (d, J_{CF} = 22.6 Hz) ppm. R_f = 0.11 (light petrol : DCM 10 : 1). Mp = 201.5 – 203.5 °C. MS (MALDI-TOF): calcd for $C_{40}H_{26}F_4N_2S$: 642.1753; found: 642.1710.

General procedure for the synthesis of **BCNA-1T** and **BSO₂MA-1T** according to Davey *et al.*[6] and Gorvin *et al.*[7] Under an argon atmosphere 4,4'-(2,5-thiophenediyl)bis(benzenamine) **3** (1 eq.), substituted fluorobenzene **4a** or **4b** (4.4 eq.) and KOtBu (4.2 eq.) were stirred in 10 mL DMSO (stored over molecular sieve, 3 Å) at 110 °C for 40 h. Conversion was monitored by TLC. The solvent was removed under reduced pressure and the remaining crude product dissolved in chloroform. After washing with water, the organic layer was dried over anhydrous sodium sulfate and evaporated to dryness under reduced pressure. Further purification was achieved by column chromatography.

4,4',4'',4'''-[2,5-Thiophenediylbis(4,1-phenylene)dinitrilo]tetrakis-[benzonitrile] (**BCNA-1T**). According to the general procedure **BCNA-1T** was synthesized applying **3** (133 mg, 0.5 mmol), KOtBu (236 mg, 2.1 mmol) and **4a** (266 mg, 2.2 mmol). After general workup the crude product was purified by column chromatography (40 g silica gel, light petrol : ethyl acetate, 5 : 1) yielding **BCNA-1T** (109 mg, 33%) as brown powder. ^{1}H NMR (400 MHz, $CDCl_3$): δ = 7.65 (d, J = 8.5 Hz, 4 H), 7.56 (d, J = 8.8 Hz, 8 H), 7.33 (s, 2 H), 7.16 (d, J = 8.6 Hz, 12 H) ppm. ^{13}C NMR (100 MHz, $CDCl_3$): δ = 150.5 (s), 145.1 (s), 143.3 (s), 134.2 (d), 132.4 (s), 127.7 (d), 127.6 (d), 125.1 (d), 123.8 (d), 119.4 (s), 106.6 (s) ppm. $R_f = 0.45$ (DCM). MS (MALDI-TOF): calcd for $C_{44}H_{26}N_6S$: 670.1940; found: 670.333.

4,4'-(2,5-Thiophenediyl)bis[*N,N*-bis[4-(methylsulfonyl)phenyl]-benzenamine] (**BSO$_2$MA-1T**). According to the general procedure **BSO$_2$MA-1T** was synthesized applying **3** (133 mg, 0.5 mmol), KOtBu (236 mg, 2.1 mmol) and **4b** (383 mg, 2.2 mmol). After general workup the crude product was purified by column chromatography (40 g silica gel, Et_2O : DCM, 1 : 3) yielding **BSO$_2$MA-1T** (184 mg, 42%) as brown powder. ^{1}H NMR (400 MHz, CD_2Cl_2) δ = 7.81 (d, J = 8.7 Hz, 8 H), 7.67 (d, J = 8.7 Hz, 4 H), 7.34 (s, 2 H), 7.26 (d, J = 8.7 Hz, 8 H), 7.20 (d, J = 8.7 Hz, 4 H), 3.06 (s, 12 H) ppm. ^{13}C NMR (100 MHz, CD_2Cl_2): δ = 151.6 (s), 145.3 (s), 143.3 (s), 135.2 (s), 132.4 (s), 129.6 (d), 127.6 (d), 127.5 (d), 125.1 (d), 123.8 (d), 45.1 (q) ppm. $R_f = 0.80$ (DCM : MeOH 10 : 1). HR-ESI-FTMS $[M+H]^+$ m/z calcd. 883.1305 for $C_{44}H_{39}N_2O_8S_5^+$, found 883.1321.

B) NMR Spectra

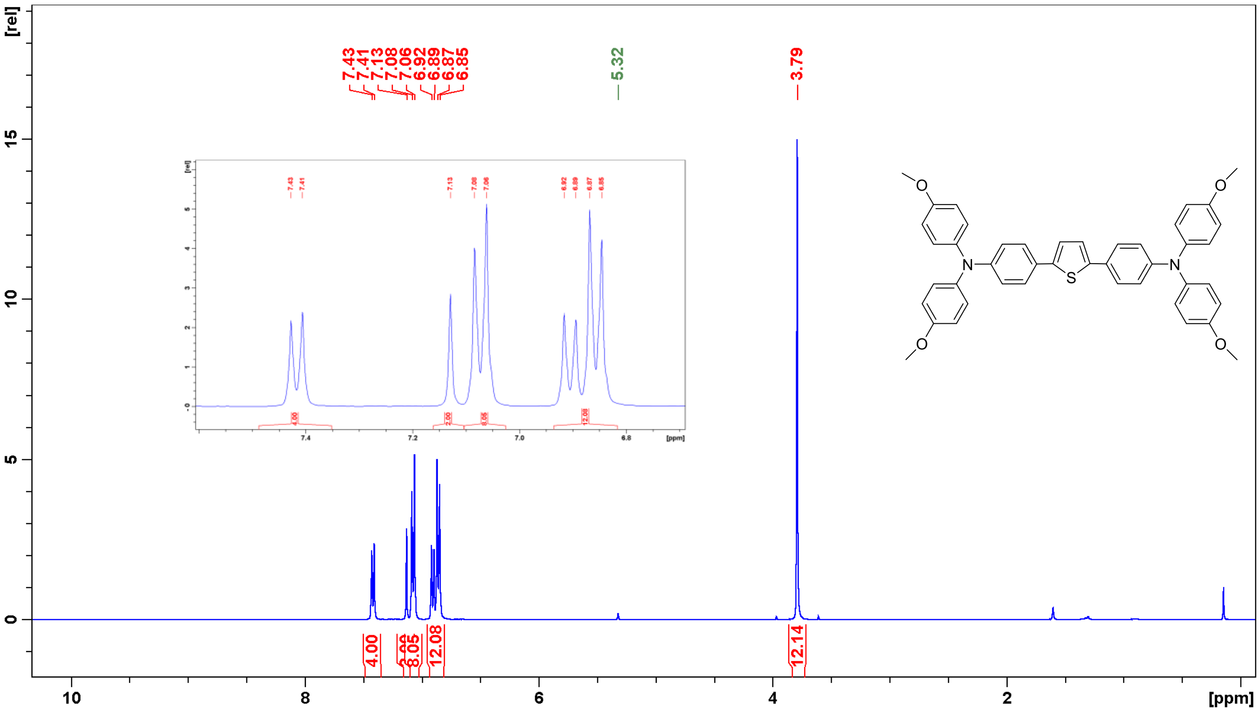

Fig. S1. Proton NMR spectrum of compound **BMOA-1T**.

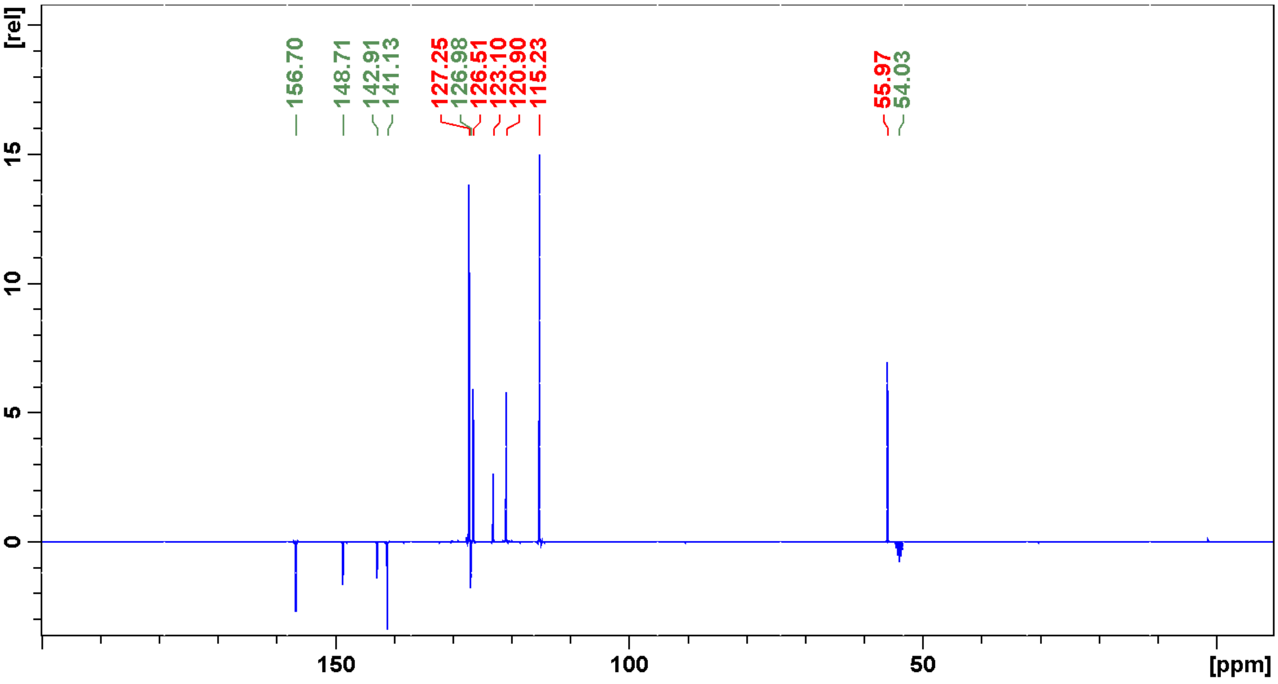

Fig. S2. Carbon NMR spectrum of compound **BMOA-1T**.

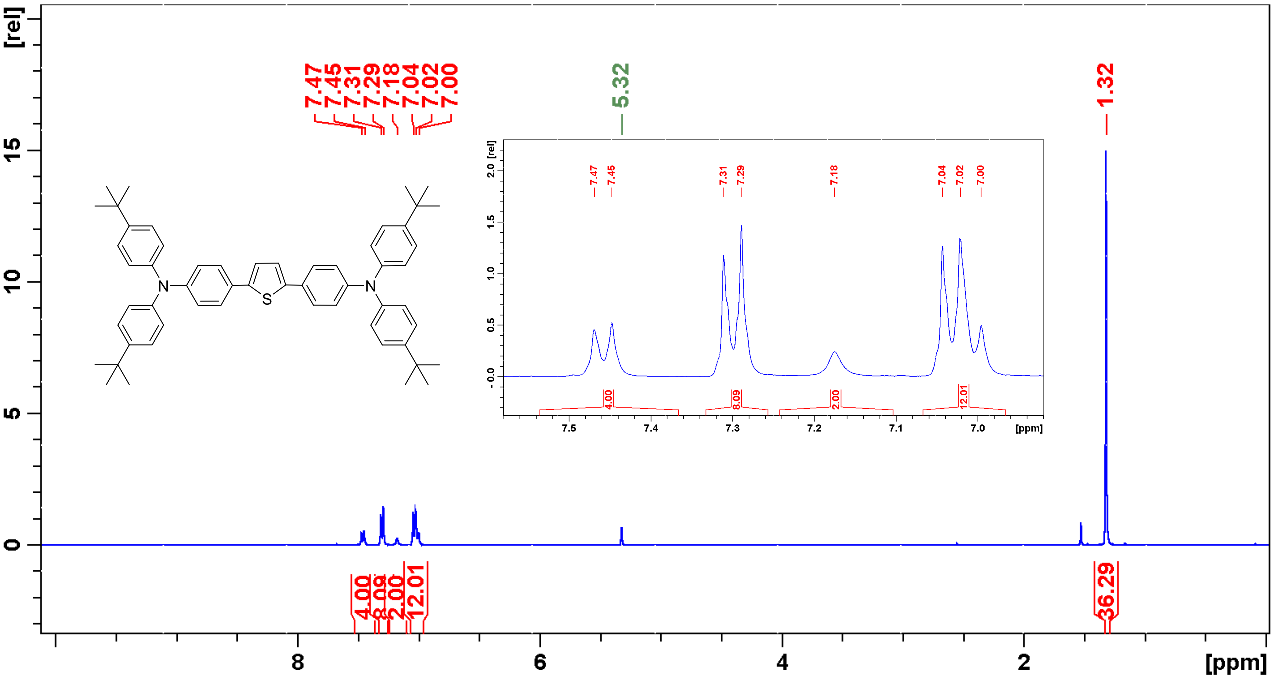

Fig. S3. Proton NMR spectrum of compound **BtBuA-1T**.

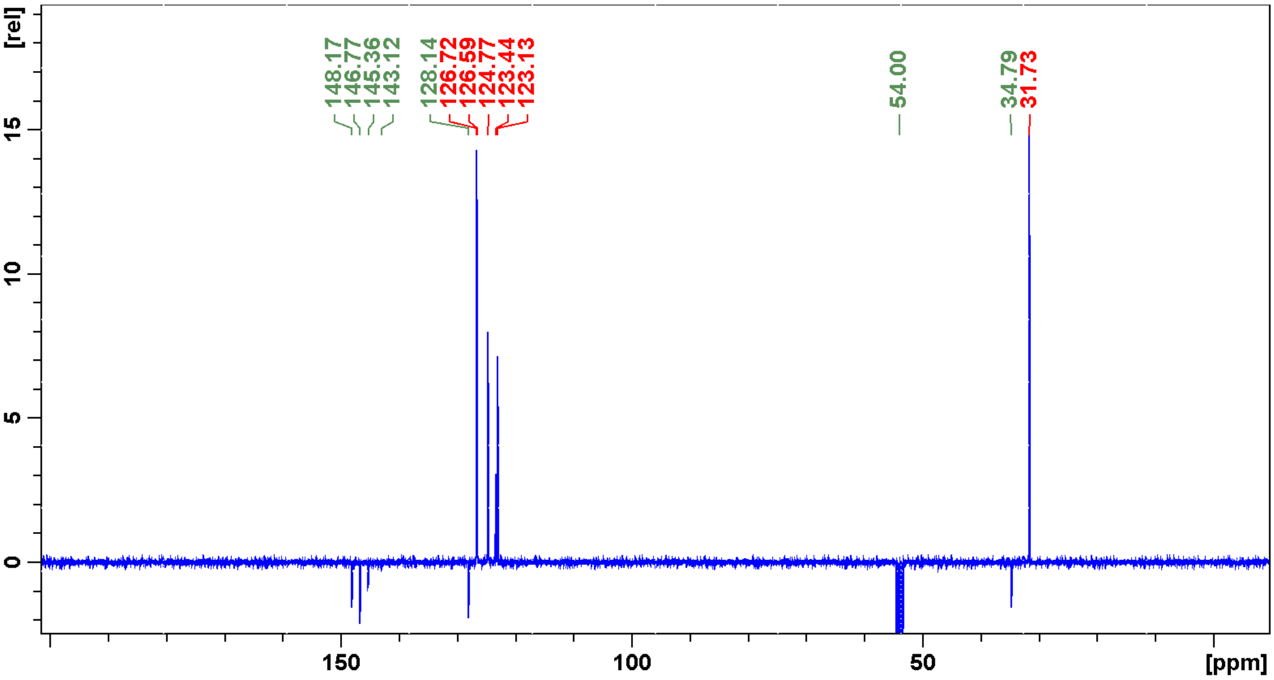

Fig. S4. Carbon NMR spectrum of compound **BtBuA-1T**.

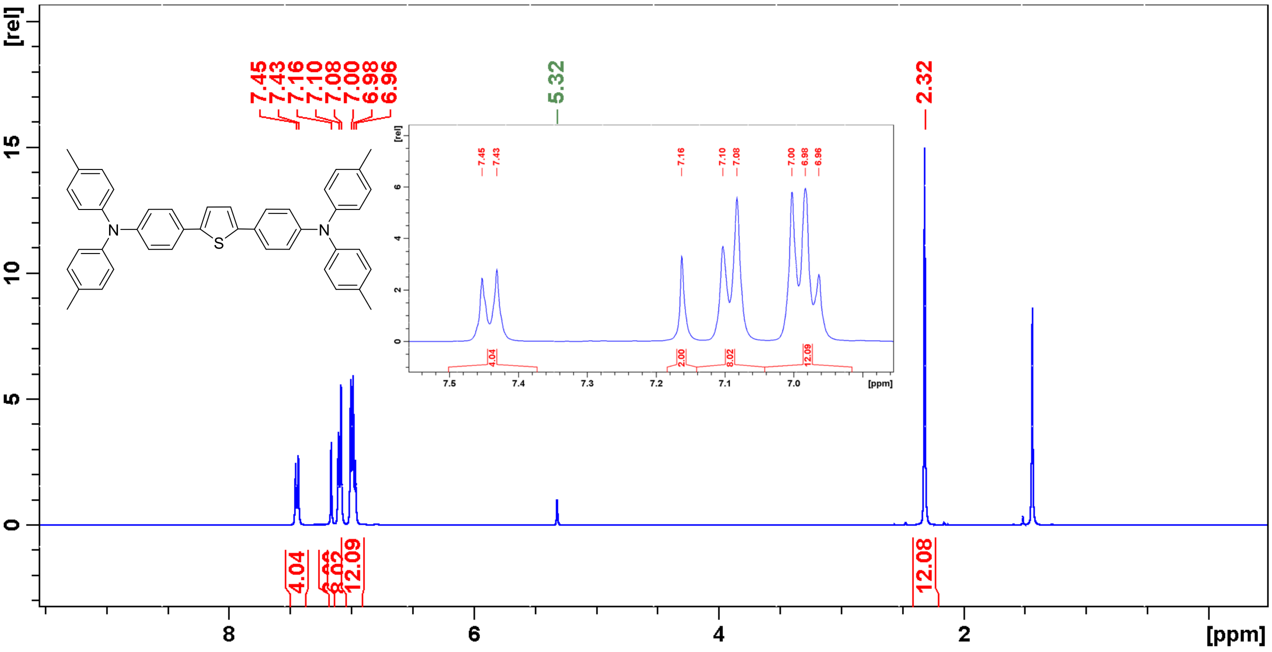

Fig. S5. Proton NMR spectrum of compound **BMA-1T**.

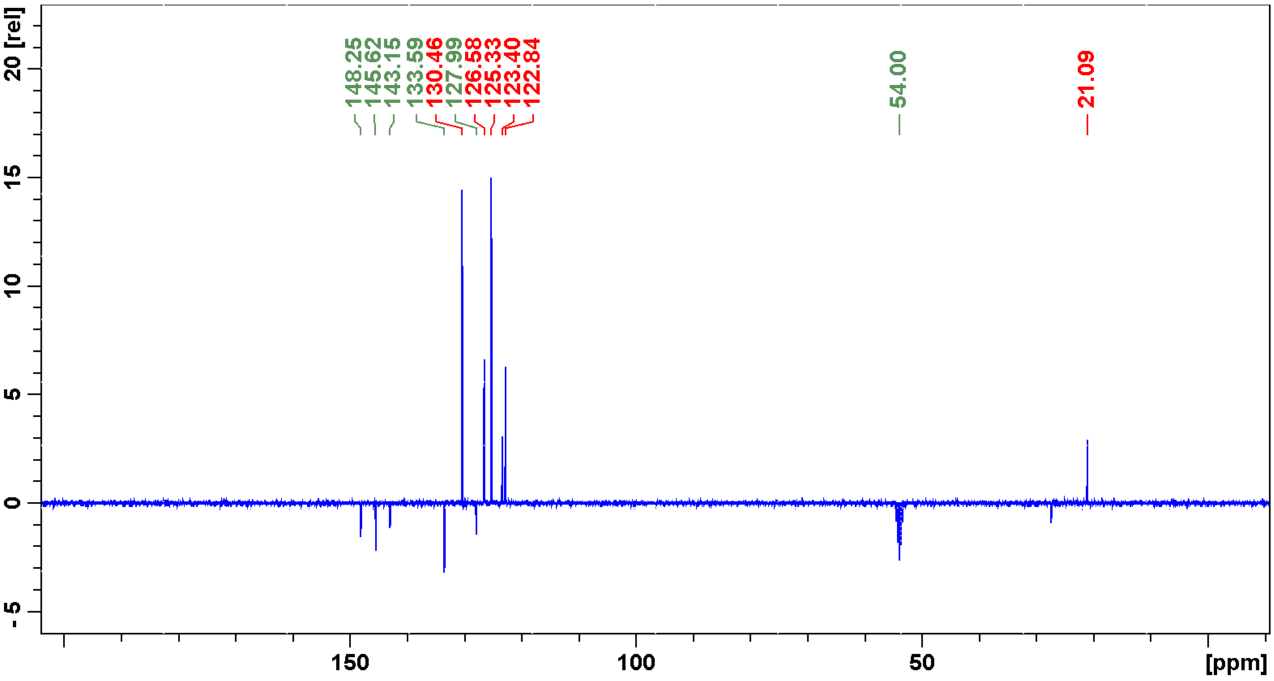

Fig. S6. Carbon NMR spectrum of compound **BMA-1T**.

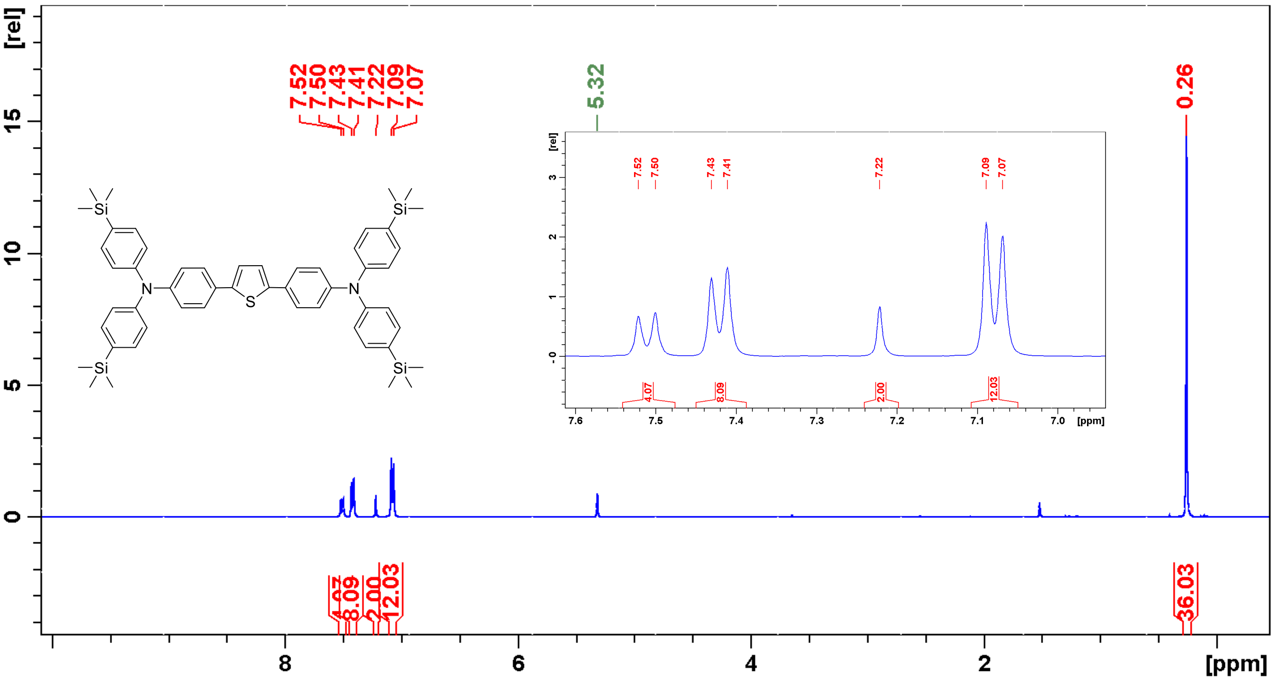

Fig. S7. Proton NMR spectrum of compound **BTMSA-1T**.

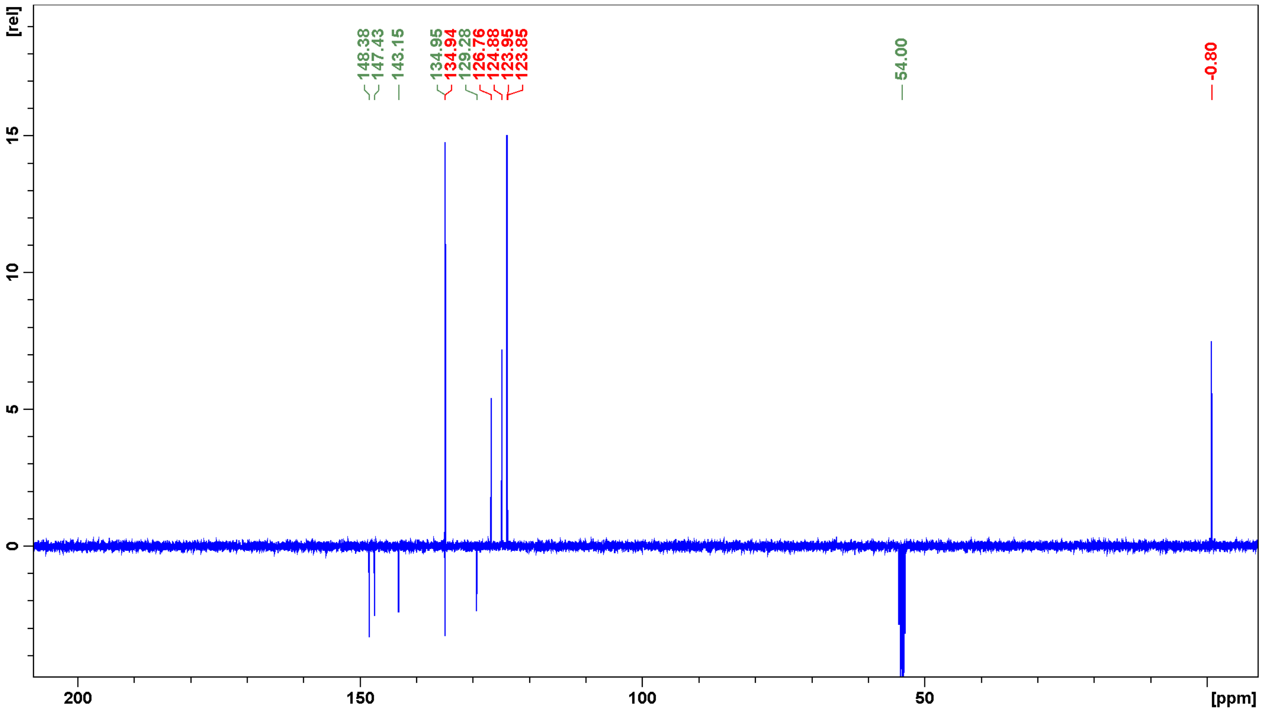

Fig. S8. Carbon NMR spectrum of compound **BTMSA-1T**.

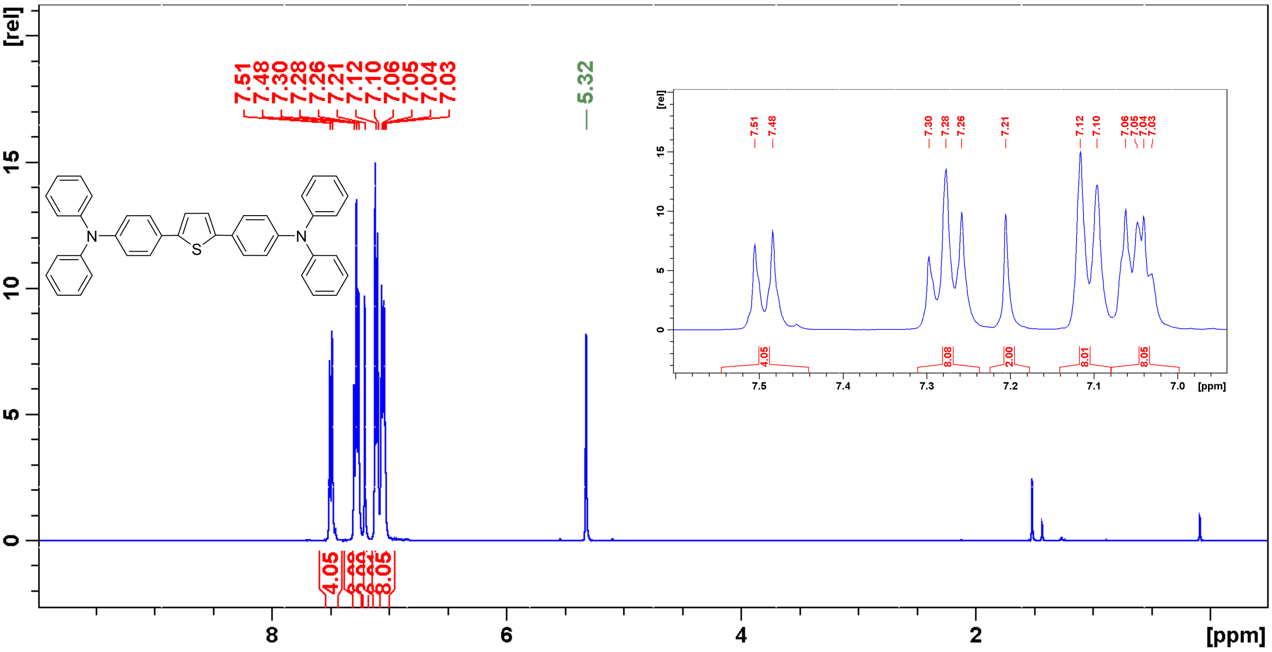

Fig. S9. Proton NMR spectrum of compound **BHA-1T**.

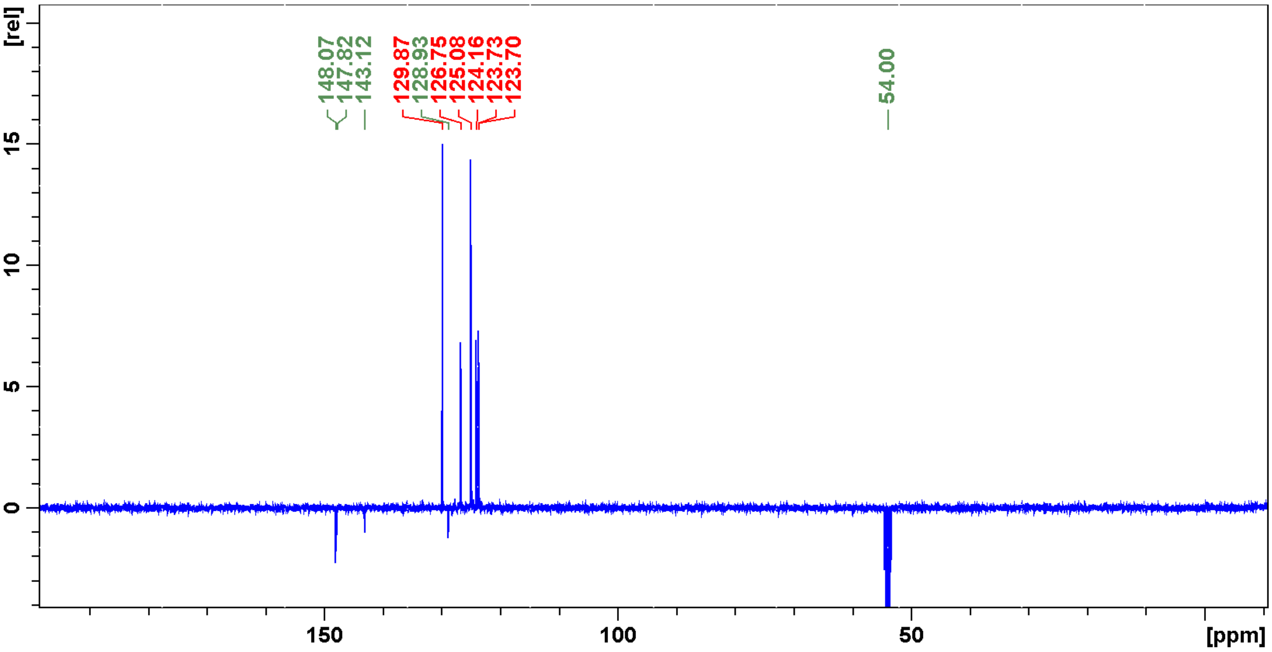

Fig. S10. Carbon NMR spectrum of compound **BHA-1T**.

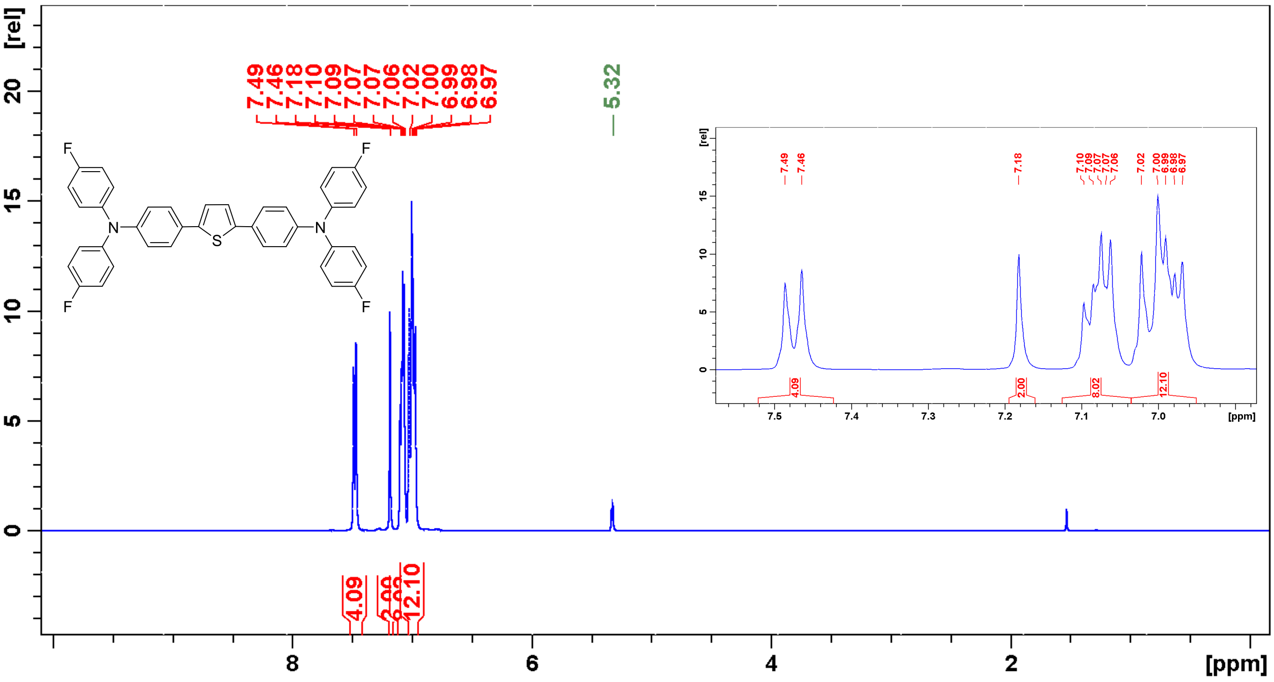

Fig. S11. Proton NMR spectrum of compound **BFA-1T**.

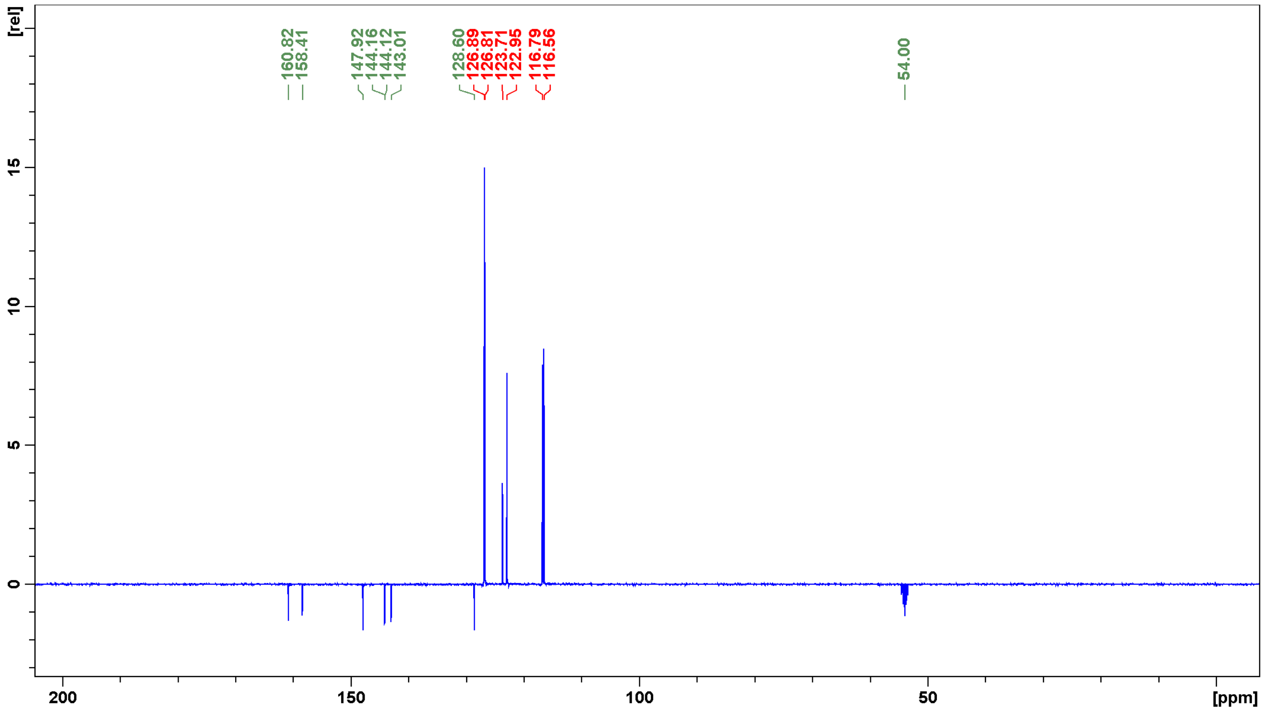

Fig. S12. Carbon NMR spectrum of compound **BFA-1T**.

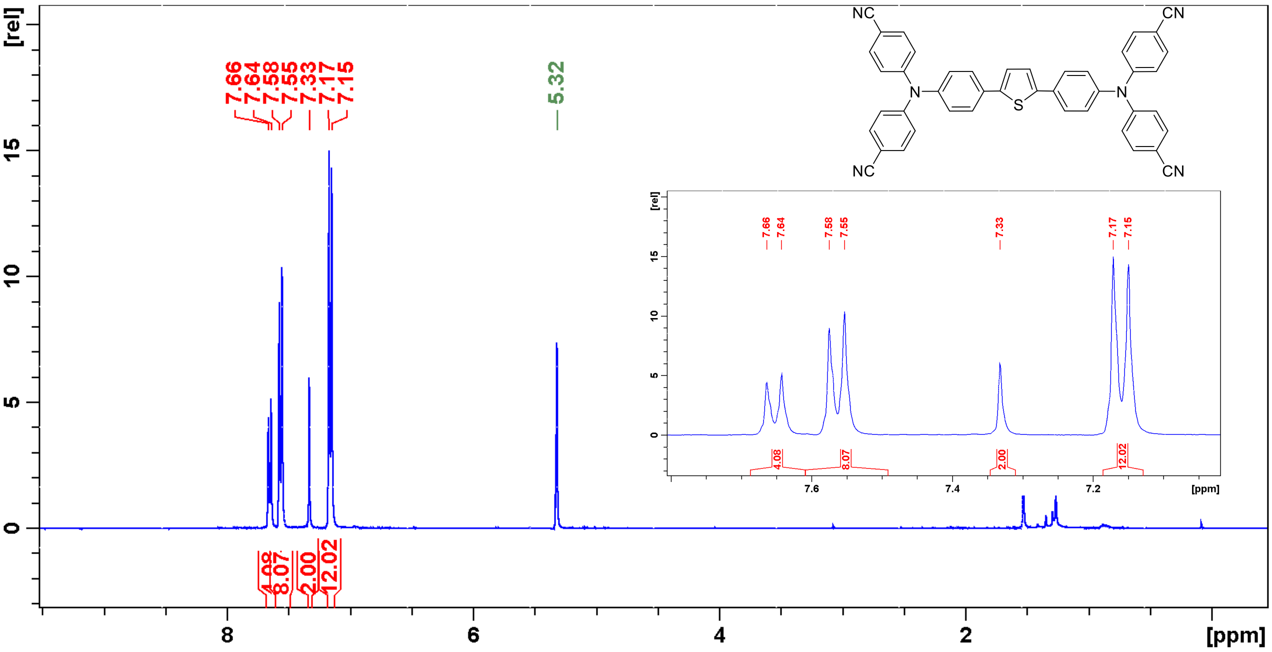

Fig. S13. Proton NMR spectrum of compound **BCNA-1T**.

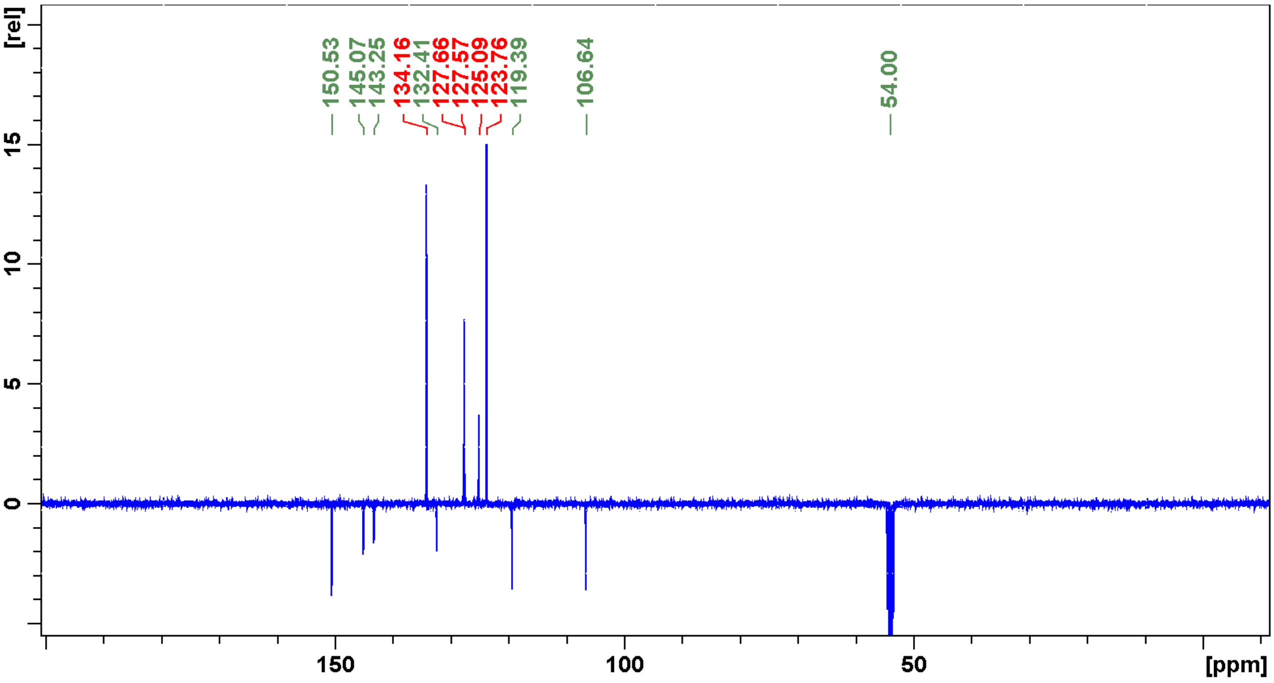

Fig. S14. Carbon NMR spectrum of compound **BCNA-1T**.

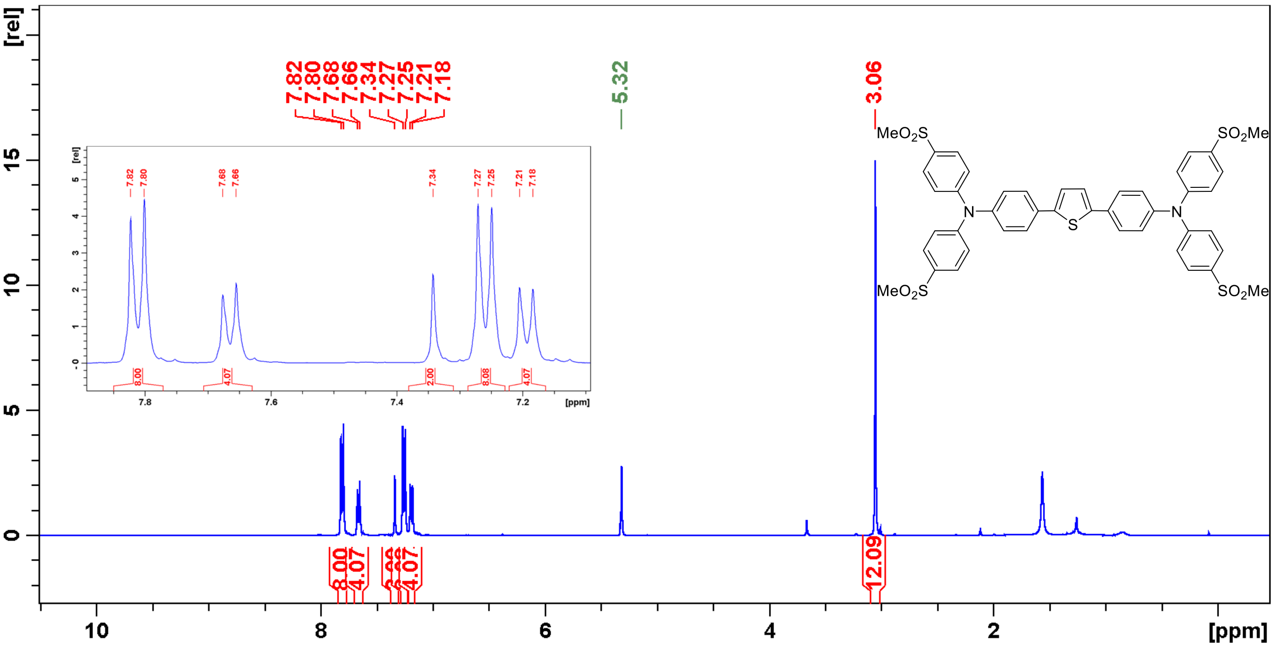

Fig. S15. Proton NMR spectrum of compound **BSO2MA-1T**.

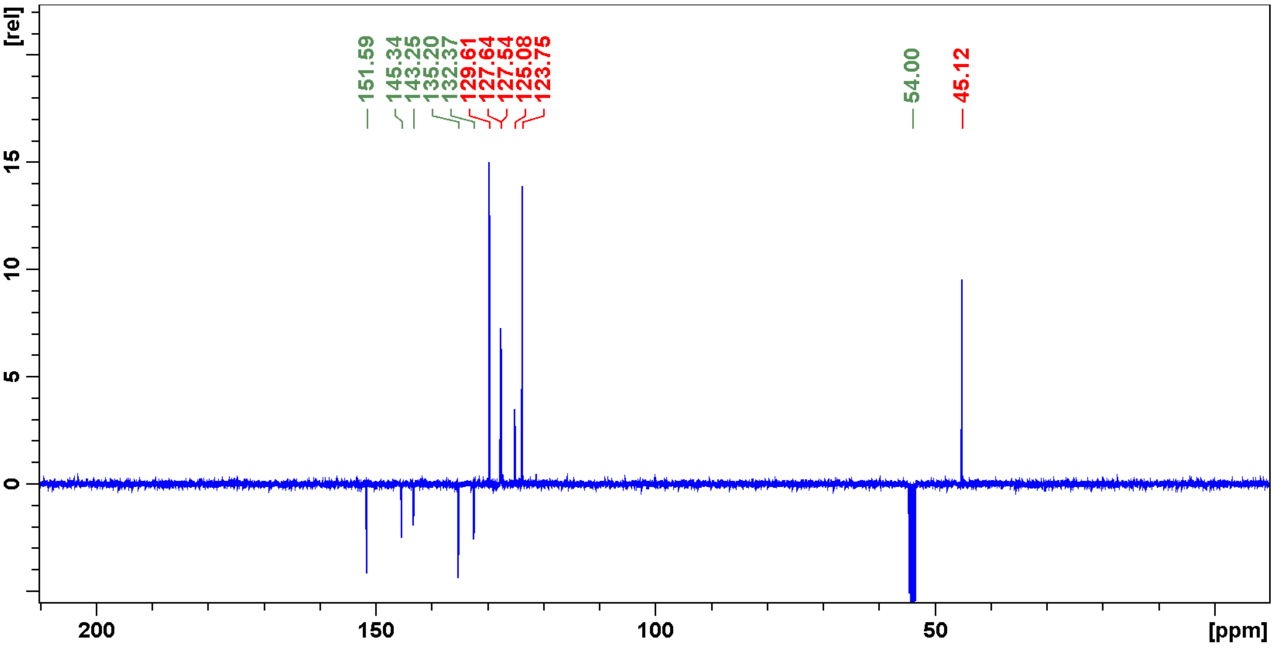

Fig. S16. Carbon NMR spectrum of compound **BSO2MA-1T**.

C) Spectroscopic Characteristics

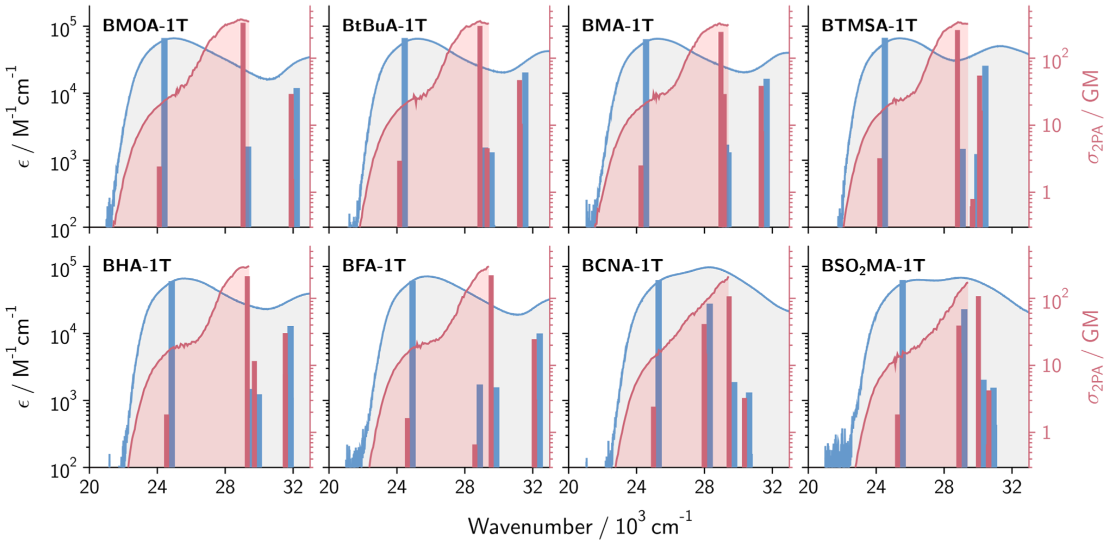

Fig. S17. One- (blue) and two-photon (red) absorption spectra on a logarithmic scale. The calculated stick spectra have been red-shifted by 4400 cm^{-1} and a single common scaling factor for 1PA and 2PA (4.4) has been applied.

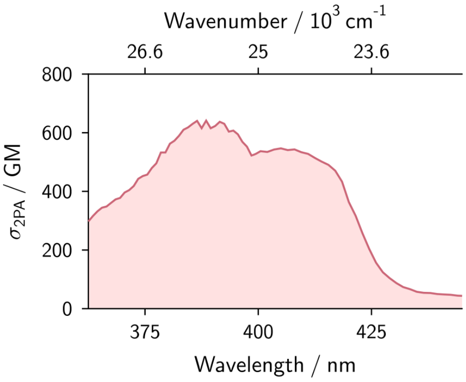

Fig. S18. Two-photon absorption spectrum of **B3FL** measured in n-hexane.

All-Optical Approach for Determining the Molar Extinction Coefficient, ε

A precise determination of the molar extinction coefficient, ε, of a compound usually relies on the application of Lambert-Beer's law, resulting in measuring absorption spectra of a series of differently concentrated samples. In order to perform these measurements with as little as possible systematic error, individual sample concentrations are usually required, while merely using a dilution series from a single stock solution is strongly discouraged. Evidently the required amount of material is rather high (at least tens of mg).

Thus, in order to work with the minimum amount of material (sub-mg), we opted for an alternative approach. In analogy to Drobizhev *et al.*[8] an all-optical determination of the extinction coefficient, ε, based on the Strickler-Berg relation is used. This approach is based on the assumption that the lowest energy absorption and emission transition moment are equal.[9] At first sight this may seem to be a bold assumption given the obvious lack of mirror symmetry for all samples even in apolar solvents, such as n-hexane. However, ultrafast broadband fluorescence experiments[10] have shown that the fluorescence transition dipole moment of **BFA-1T** and **BMOA-1T** in nonpolar solvents changes only marginally from its Franck-Condon value, which should be identical to the transition dipole moment of absorption. The procedure for obtaining ε was thus as follows:

1. Determine the transition dipole moment of fluorescence, μ_{01} eq. (S1), in apolar cyclohexane.
2. Decompose the lowest energy absorption band into the two excitonic bands applying displaced harmonic oscillator line shape functions (eq. (S2); cf. Fig. S19)
3. Evaluate the absorption spectrum scaling factor by equaling the transition dipole moment for the lowest energetic absorption band, μ_{10} (eq. (S3)) with the emission one, μ_{01}, in n-hexane.

Errors introduced by the not unambiguous decomposition (point 2) are expected to not exceed approx. 10%.

In this context it is important to note, that

a) with the exception of **BMOA-1T** the experimental emission TDMS, μ_{01}, are solvent-independent

b) the μ_{01} of all investigated compounds are virtually identical (for **BMOA-1T** this is only true for the value measured in n-hexane; its reduction in more polar solvents for **BMOA-1T** can be ascribed to excited state symmetry breaking)

$$\mu_{01} = 1785.7\sqrt{\frac{k_{\mathrm{r}}}{n f_n^2}\frac{\int F(\tilde{\nu})\tilde{\nu}^{-3}\mathrm{d}\tilde{\nu}}{\int F(\tilde{\nu})\mathrm{d}\tilde{\nu}}} \qquad \text{(S1)}$$

$$\mathrm{A}(\tilde{\nu}) \propto \tilde{\nu}\sum_{i=1}^{3}\left(\sum_{m=0}^{\infty}\frac{S_i^m e^{-S_i}}{m!}\exp\left(-\frac{(h\tilde{\nu}_i^0 + m\hbar\omega_i - h\tilde{\nu})^2}{2\sigma_i^2}\right)\right) \qquad \text{(S2)}$$

$$\mu_{10} = 9.584\cdot 10^{-2}\sqrt{\frac{n}{f_n^2}\int\frac{\epsilon_{S_1}(\tilde{\nu})}{\tilde{\nu}}\mathrm{d}\tilde{\nu}} \qquad \text{(S3)}$$

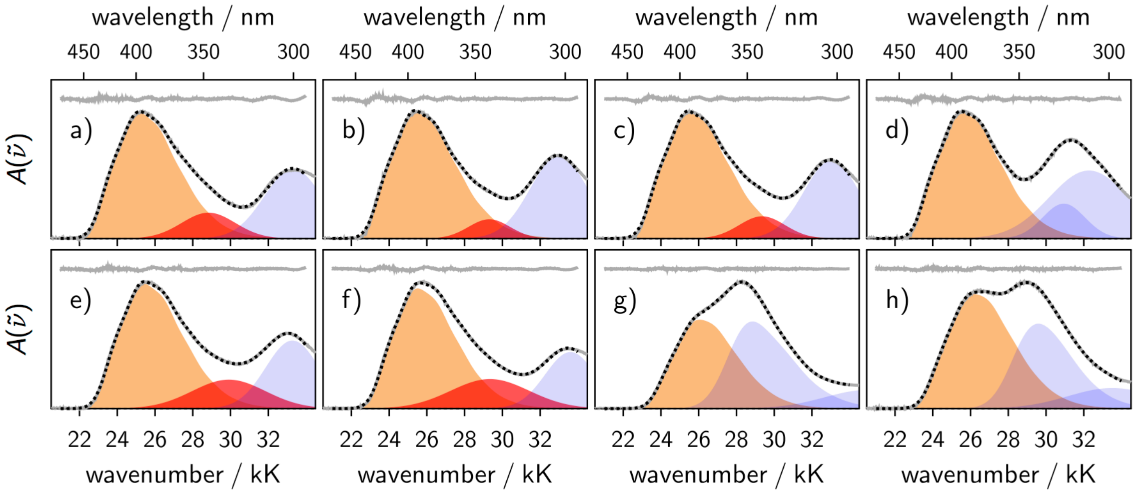

Fig. S19. Absorption spectra in n-hexane (a-d) and THF (e-h), (**BMOA-1T**, **BtBuA-1T**, **BMA-1T**, **BTMSA-1T**, **BHA-1T**, **BFA-1T**, **BCNA-1T**, **BSO₂MA-1T**). The spectra have been decomposed according to eq. (S3), with the orange spectrum denoting the lowest energy transition from which μ_{10} is calculated. The red spectrum cannot be assigned unambiguously for d), g) and h) where significant overlap with the local TPA transition is observed. The offset grey line denotes the residuals between the decomposition (dashed black line) and the experimental data (grey line).

D) Quantum Chemical Calculations

	E [1000 cm^{-1}]	μ_{x0} [D]	$<\delta^{TPA}_{a.u.}>$
BMOA-1T	28.82	11.68	334.23
	32.73	0.19	0.32
	32.75	2.07	1121.99
	33.75	1.81	39851.49
	36.59	0.19	3184.55
	36.61	4.95	170.19
	37.23	0.60	278.03
BtBuA-1T	28.86	11.68	404.81
	33.59	1.78	35912.33
	33.97	1.64	3.13
	34.01	0.47	533.01
	35.92	1.81	5220.17
	35.96	6.46	1164.83
	38.13	0.91	388.62
BMA-1T	28.96	11.45	345.42
	33.67	1.87	29127.58
	33.81	1.64	2.63
	33.86	0.31	3431.02
	36.04	1.64	4268.93
	36.06	5.80	892.54
	38.13	1.08	253.29
BTMSA-1T	28.91	11.72	440.23
	33.49	1.74	31265.59
	34.36	1.59	72.17
	34.39	0.72	92.42
	34.79	2.33	6290.99
	34.83	7.25	1888.65
	38.27	0.54	917.07
BHA-1T	29.25	11.10	254.18
	34.00	1.74	25013.78
	34.38	1.59	0.55
	34.42	0.27	1337.82
	36.24	1.50	3323.95
	36.25	5.13	802.26
	38.60	0.91	312.81
BFA-1T	29.32	11.16	219.46
	33.28	1.88	10.82
	33.29	0.15	77.06
	34.25	1.79	25682.23
	36.79	1.11	2669.08
	36.81	4.52	334.54
	37.94	1.11	369.41
BCNA-1T	29.70	11.32	326.92
	32.68	3.43	5029.13
	32.71	7.54	1821.09
	34.15	1.96	12491.25
	35.03	1.64	22.81
	35.06	0.57	371.41
	38.06	0.13	2107.18
BSO2MA-1T	29.96	11.33	246.89
	33.57	3.34	4652.61
	33.59	6.86	1811.33
	34.72	2.04	12338.71
	35.31	1.78	74.44
	35.34	0.94	475.53
	38.55	0.30	1897.97

Table S1. Summary of one- and two-photon properties for all compounds obtained using DFT calculations based on long-range corrected hybrid CAM-B3LYP functional and the cc-pVDZ basis set.

The integrated one-photon extinction coefficient of transition x, $\epsilon_{\mathrm{int},x}$, can be directly obtained from the transition dipole moments, μ_{x0} (in Debye) according to Arzhantsev[11] and Toptygin[12]

$$\epsilon_{\mathrm{int},x} = \int_x \frac{\epsilon(\omega)}{\omega}\mathrm{d}\omega = \frac{\mu_{x0}^{\;2}}{9.158\times10^{-3}}\frac{f_n^{\;2}}{n},$$

where n denotes the solvent refractive index and f_n is the local field correction factor and in the framework of the empty spherical cavity model is given as $f_n = 3n^2/(2n^2+1)$.

The two-photon absorption cross section spectra in GM, $\sigma(\omega)$, are usually calculated from $\langle\delta_{\mathrm{a.u.}}^{\mathrm{TPA}}\rangle$ following reference[13]

$$\sigma(\omega) = \frac{8\pi^3\alpha a_0^5\omega^2}{c}\langle\delta_{\mathrm{a.u.}}^{\mathrm{TPA}}\rangle g(2\omega,\omega_0,\Gamma),$$

with the numerical values given in ref.[14]. The lineshape function so defined is normalized to 0.5 by integration over ω. Rather than calculating spectra and in line with the one-photon approach, we opted for obtaining integrated two-photon extinction coefficient of transition x, $\sigma_{\mathrm{int},x}$. This quantity for each transition can be directly obtained from the Dalton output in Table S1 using:

$$\sigma_{\mathrm{int},x} = \int_x \frac{\sigma(\omega)}{\omega}\mathrm{d}\omega \frac{4\pi^3\alpha a_0^5\omega}{c}\langle\delta_{\mathrm{a.u.}}^{\mathrm{TPA}}\rangle_x.$$

Fig. S20-S25 show the optimized structures and molecular orbitals (MO) involved in the formation of lowest excited states of the studied 2PA PIs calculated in THF at M06-2X/6-31G(d,p)/PBF level of theory.

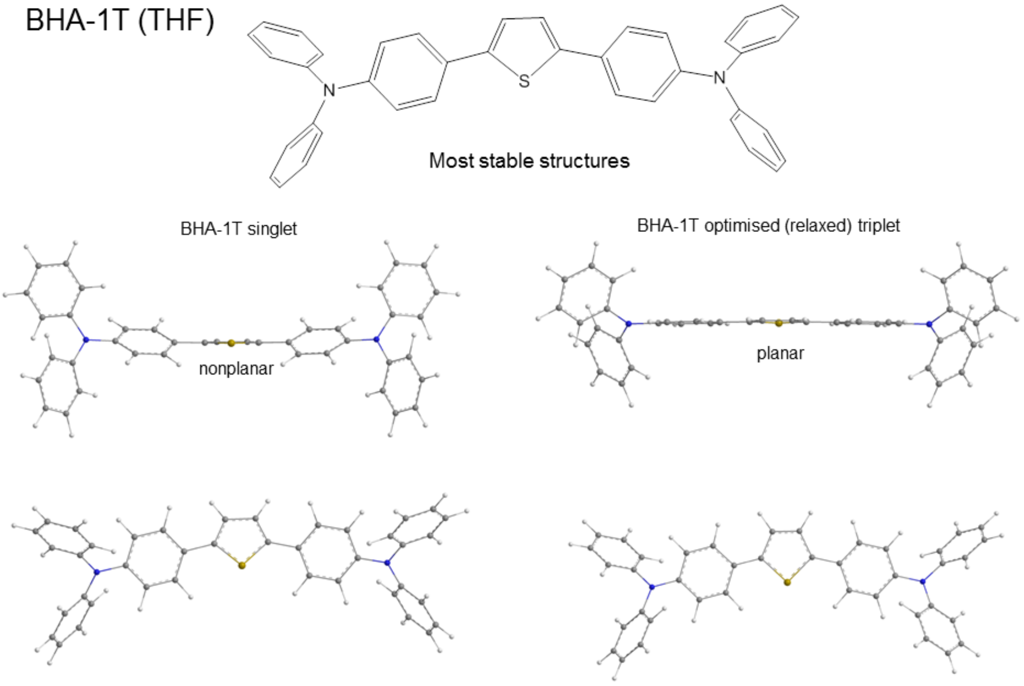

Fig. S20. Optimized structures of ground state singlet S_0 and optimized (relaxed) triplet T_1 of **BHA-1T**.

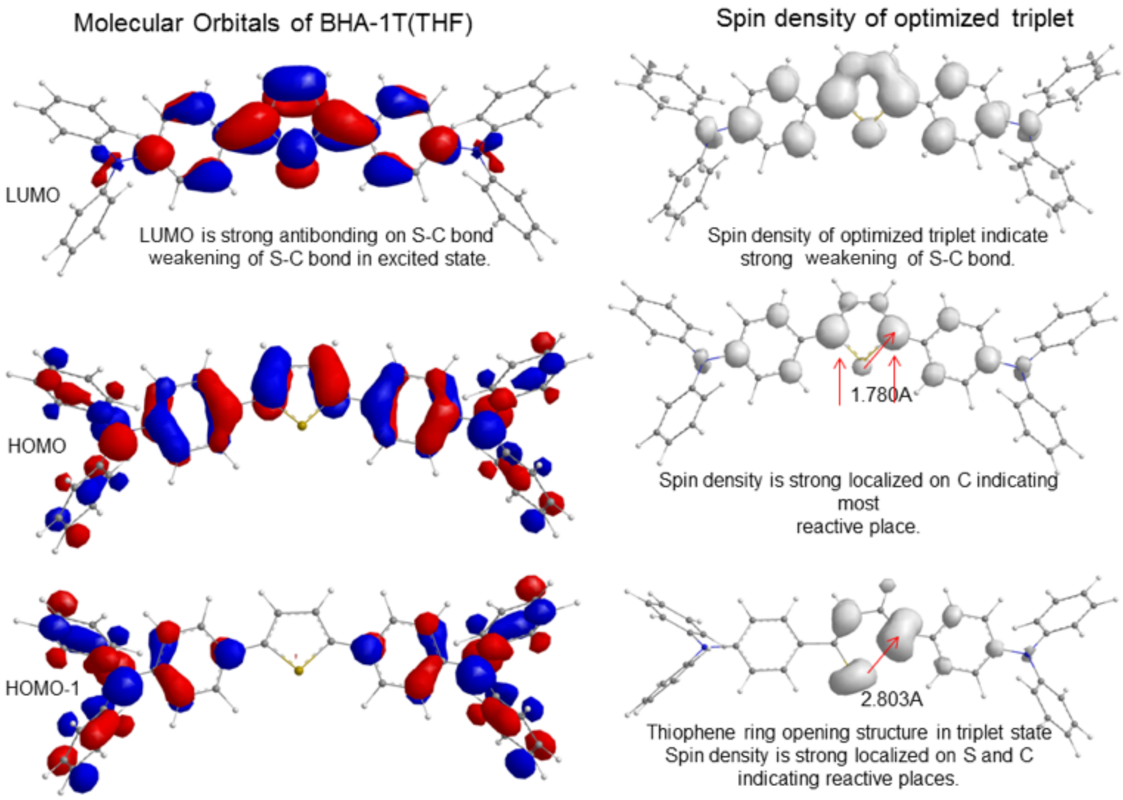

Fig. S21. Molecular orbitals of ground state singlet S_0 and spin density distribution of optimized triplet T_1 of **BHA-1T**.

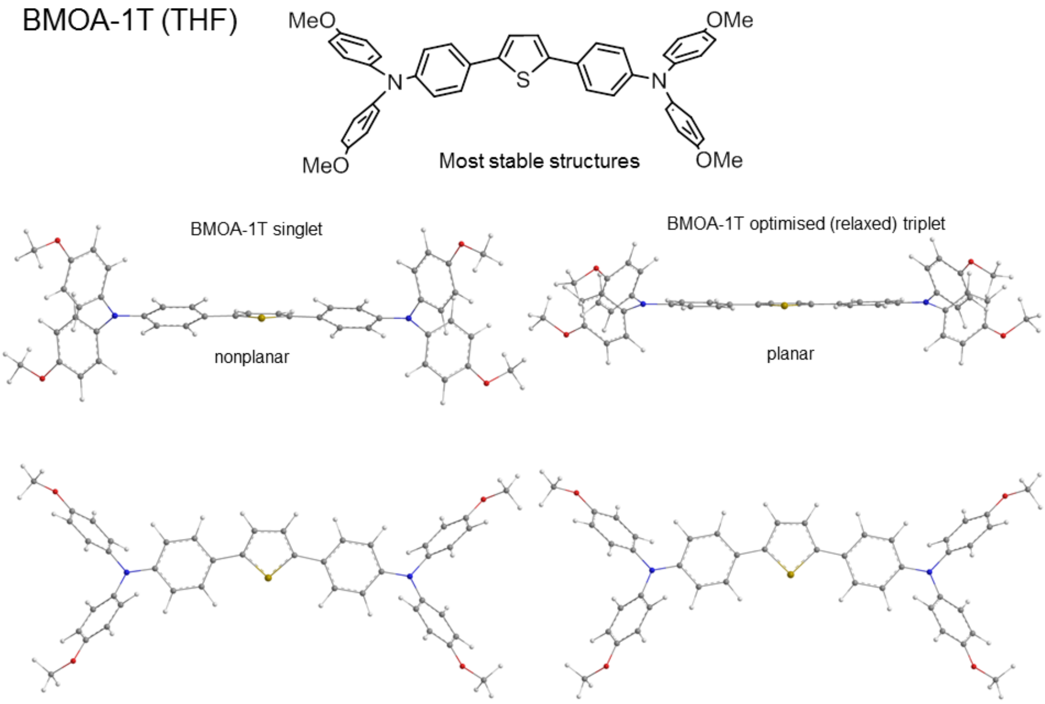

Fig. S22. Optimized structures of ground state singlet S$_0$ and optimized (relaxed) triplet T$_1$ of **BMOA-1T**.

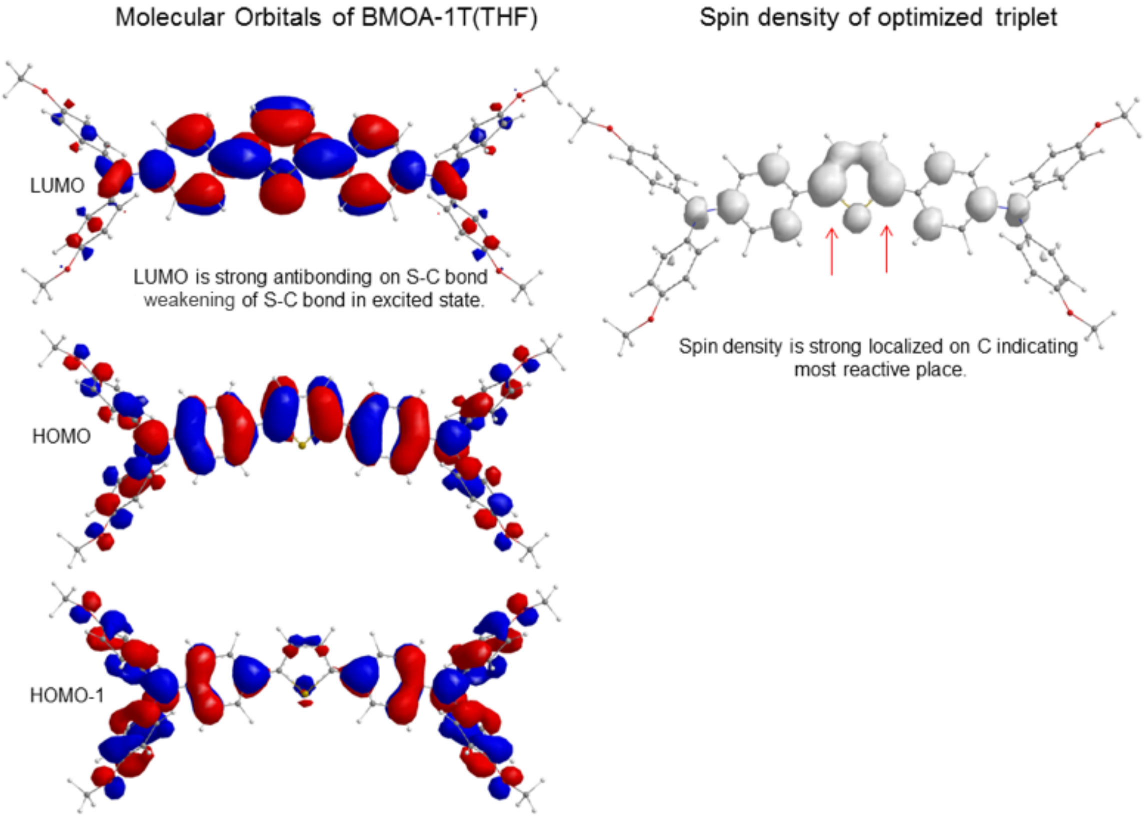
Molecular Orbitals of BMOA-1T(THF)

Spin density of optimized triplet

LUMO is strong antibonding on S-C bond weakening of S-C bond in excited state.

Spin density is strong localized on C indicating most reactive place.

Fig. S23. Molecular orbitals of ground state singlet S$_0$ and spin density distribution of optimized triplet T$_1$ of **BMOA-1T**.

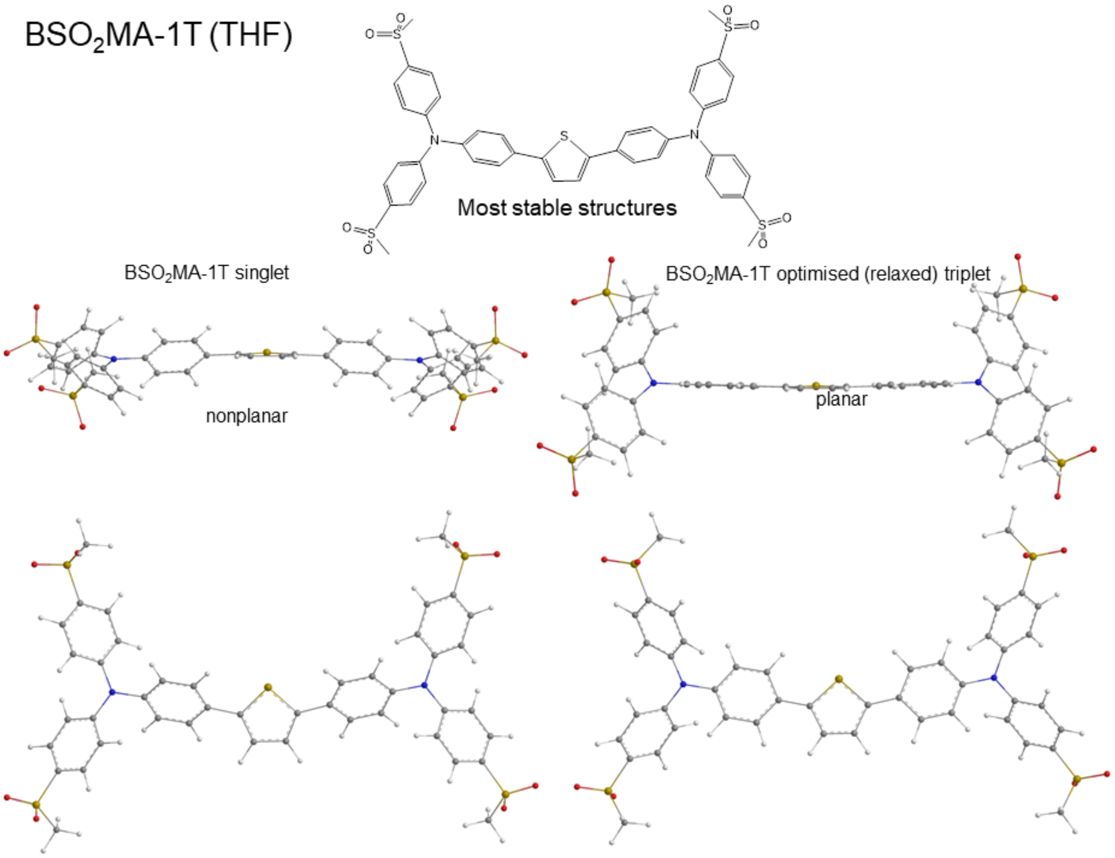

Fig. S24. Optimized structures of ground state singlet S_0 and optimized (relaxed) triplet T_1 of **BSO$_2$MA-1T**.

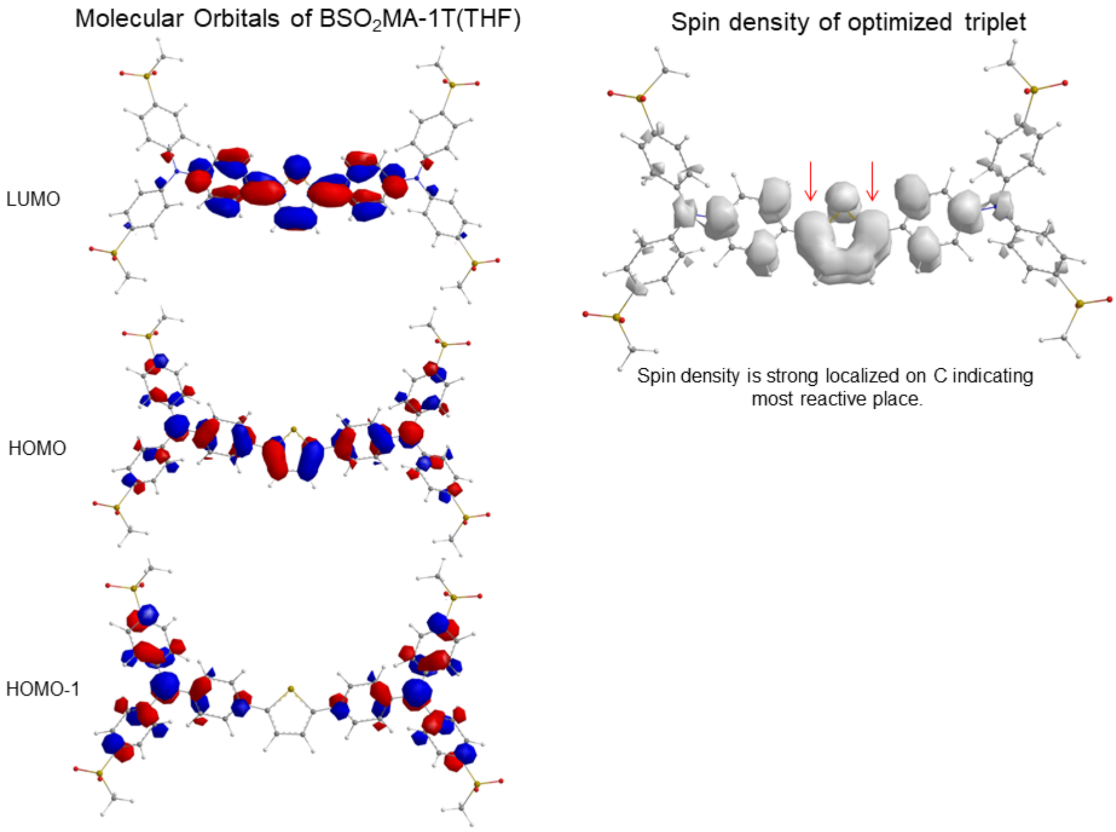

Fig. S25. Molecular orbitals of ground state singlet S_0 and spin density distribution of optimized triplet T_1 of **BSO$_2$MA-1T**.

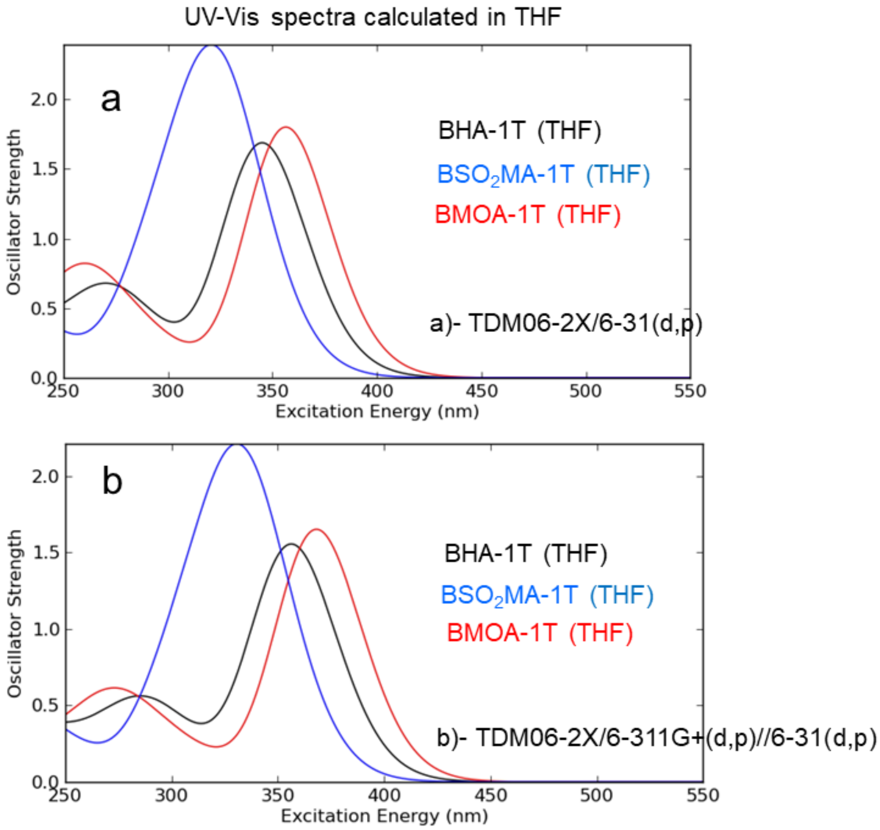

Fig. S26. Absorption spectra of the studied 2PA PIs in THF calculated at the two levels of theory.

E) 2PA Screening Tests

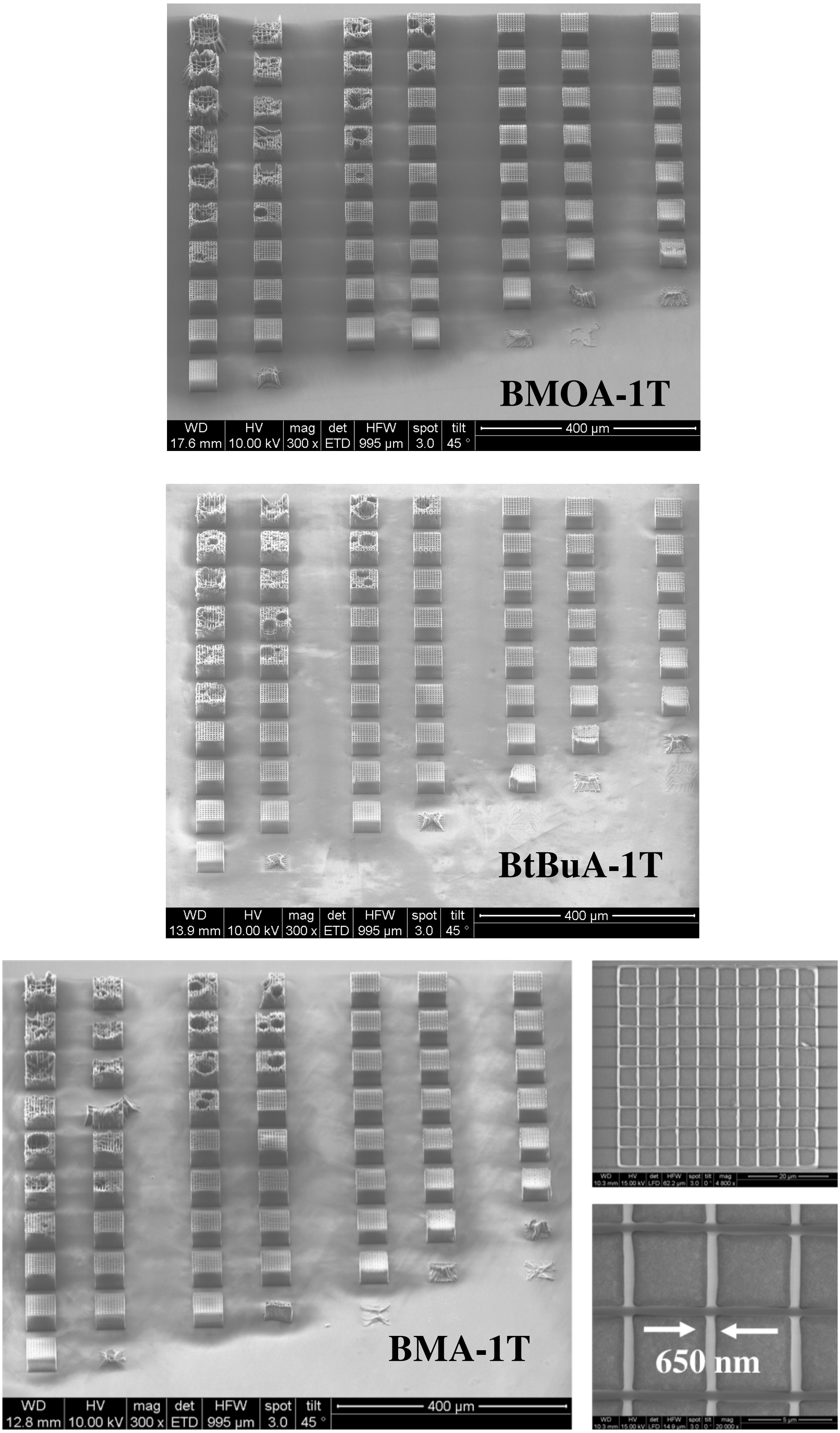

Figure S27. 2PP structuring test of **BMOA-1T**, **BtBuA-1T** and **BMA-1T** as well as magnification of woodpiles of a test series using **BMA-1T**.

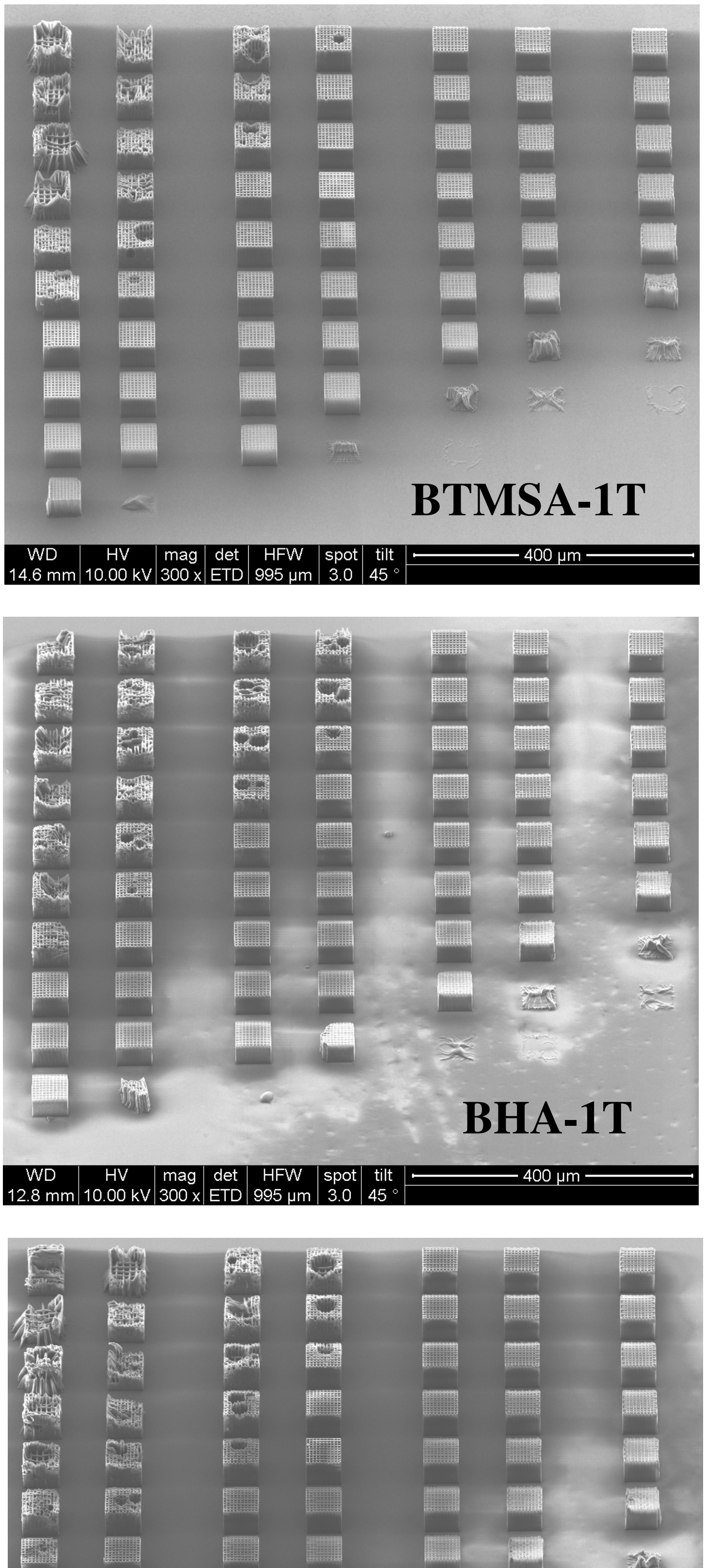

Figure S28. 2PP structuring test of **BTMSA-1T**, **BHA-1T** and **BFA-1T**.

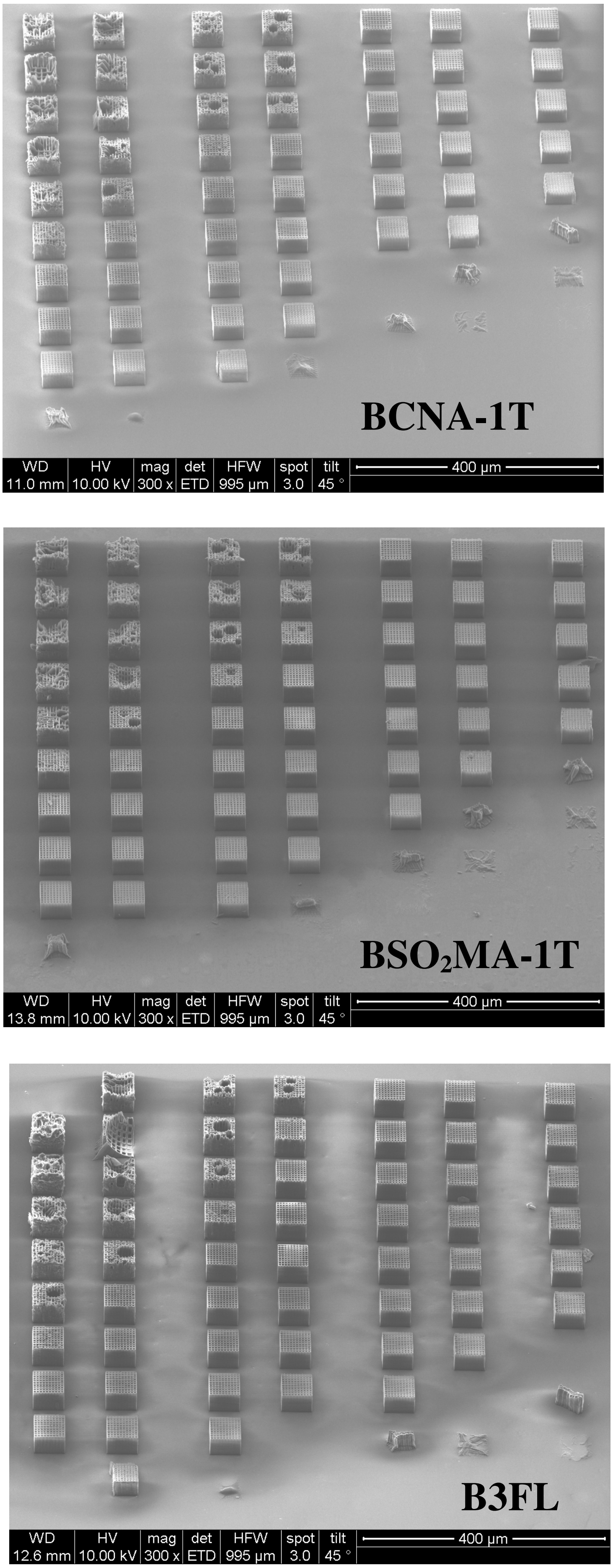

Figure S29. 2PP structuring test of **BCNA-1T**, **BSO$_2$MA-1T** and **B3FL**.

F) References

1 O. Navarro and S. P. Nolan, *Synthesis*, 2006, 366–367.

2 C. Almansa, J. Alfón, A. F. de Arriba, F. L. Cavalcanti, I. Escamilla, L. A. Gómez, A. Miralles, R. Soliva, J. Bartrolí, E. Carceller, M. Merlos and J. García-Rafanell, *J. Med. Chem.*, 2003, **46**, 3463–3475.

3 J. L. Gonzalez, C. E. Stephens, T. Wenzler, R. Brun, F. A. Tanious, W. D. Wilson, T. Barszcz, K. A. Werbovetz and D. W. Boykin, *Eur. J. Med. Chem.*, 2007, **42**, 552–557.

4 D. Lumpi, B. Holzer, J. Bintinger, E. Horkel, S. Waid, H. D. Wanzenböck, M. Marchetti-Deschmann, C. Hametner, E. Bertagnolli, I. Kymissis and J. Fröhlich, *New J Chem*, 2015, **39**, 1840–1851.

5 N. Marion, O. Navarro, J. Mei, E. D. Stevens, N. M. Scott and S. P. Nolan, *J. Am. Chem. Soc.*, 2006, **128**, 4101–4111.

6 M. H. Davey, V. Y. Lee, L.-M. Wu, C. R. Moylan, W. Volksen, A. Knoesen, R. D. Miller and T. J. Marks, *Chem. Mater.*, 2000, **12**, 1679–1693.

7 J. H. Gorvin, *J. Chem. Soc. Perkin 1*, 1988, 1331–1335.

8 M. Drobizhev, S. Tillo, N. S. Makarov, T. E. Hughes and A. Rebane, *J. Phys. Chem. B*, 2009, **113**, 855–859.

9 S. J. Strickler and R. A. Berg, *J. Chem. Phys.*, 1962, **37**, 814–822.

10 J. S. Beckwith, A. Rosspeintner, G. Licari, M. Lunzer, B. Holzer, J. Fröhlich and E. Vauthey, *J. Phys. Chem. Lett.*, 2017, **8**, 5878–5883.

11 S. Arzhantsev, K. A. Zachariasse and M. Maroncelli, *J. Phys. Chem. A*, 2006, **110**, 3454–3470.

12 D. Toptygin, *J. Fluoresc.*, 2003, **13**, 201–219.

13 D. H. Friese, A. Mikhaylov, M. Krzeszewski, Y. M. Poronik, A. Rebane, K. Ruud and D. T. Gryko, *Chem. - Eur. J.*, 2015, **21**, 18364–18374.

14 M. T. P. Beerepoot, D. H. Friese, N. H. List, J. Kongsted and K. Ruud, *Phys Chem Chem Phys*, 2015, **17**, 19306–19314.